

Chapter 1

Shadowing, errors, and exact orbits of quadratic maps

Jason A.C. Gallas

*Instituto de Altos Estudos da Paraíba, Rua Silvino Lopes 419-2502,
58039-190 João Pessoa, Brazil*

*Complexity Sciences Center, 9225 Collins Avenue Suite 1208,
Surfside FL 33154, USA*

*Max-Planck Institute for the Physics of Complex Systems,
Nöthnitzer Str. 38, 01187 Dresden, Germany*

Abstract: We consider two problems in dynamical systems. First, shadowing, namely the impact of small numerical errors in calculations of orbital points of the two-dimensional Hénon map is investigated. The unique map inverse allows one to access numerical errors by performing, under size-controlled representation of real numbers, a “there and back game”, namely, iterating the map arbitrarily forward and, from there, backtracking using the unique inverse. Numerical errors are determined by measuring the distance between the points of departure and return. Second, we report exact analytical results for the quadratic map in the fully chaotic partition generating limit. In particular, exact expressions for periodic orbits and for preperiodic points allow one to extract precise coordinates of points belonging to periodic orbits. Such coordinates provide valuable checkpoints against which to gauge propagation errors for some classes of numerical calculations. The simple systems considered here provide fruitful workhorses to investigate numerical noise and error propagation when performing large number of iterates.

1. Introduction

Le cose sono unite da legami invisibili. Non puoi
cogliere un fiore senza turbare una stella.
Galileo Galilei

The overwhelming majority of models that are interesting from a practical or fundamental point of view turn out to be hard to deal with numerically. This is so because it is quite difficult to numerically compute approximate solutions of an initial value problem which remain close to true solutions over a long time interval. To begin with, what should be understood by a “true solution” of a problem that cannot be integrated exactly? This question is relevant because virtually every equation of motion does not allow a solution to be represented in closed form and, therefore, to mimic the ad-hoc and very narrow class of problems which admit exact solutions and which are traditionally found in introductory textbooks of calculus and classical dynamics. Systems allowing exact analytical solutions are the exception, not the rule.

The task of solving typical equations of motion becomes generally impossible if one fixes the precision of the numerical representation of real numbers and demands solutions to remain valid over arbitrarily long time intervals. Numerical solutions normally involve hundred of thousands or even millions of iterates. To numerically solve equations of motion means to iterate discrete maps, either stepping forward a numerical integrator, or iterating a map assumed to represent the dynamics. In this context, it becomes natural to inquire about the exact meaning and significance of *numerical solutions* of equations of motion, and for how long such numerical approximations remain valid. But, how to make sense of this questions when “true” solutions are unknown and impossible to obtain? Against what can we gauge numerically obtained solutions? It is one thing for a given dynamical system to have true orbits, that may behave in complicated or even chaotic ways, and another for such orbits to be computable, or observable in real life.

To address numerical computability problems, mathematicians came up with a number of concepts and claims centered around the notion of *shadowing*, all arising from a shadowing theorem for Anosov diffeomorphisms.¹ Anosov and Bowen showed that in systems which are *uniformly hyperbolic*, approximate numerical (i.e. “noisy”) orbits will stay “close”, or shadow, a true orbit for arbitrarily long times. Note the use of “a true”, not “the true” orbit. Regrettably, a key issue in this context is that the shadowing theo-

rem does not apply to real-life systems, which tend to be never hyperbolic let alone uniformly hyperbolic. Thus, strictly, one is still left in the dark regarding true mathematical orbits, having to rely on numerical experiments and rules of thumb derived from them which, nevertheless, use to emerge dressed as theorems, with dubious significance for applications. The rigorous study of shadowability has been a surprisingly difficult and technically sophisticated mathematical playground which so far seems to have only been thoroughly carried out in the case of one-dimensional maps, like maps of intervals or the circle, or the two-dimensional Hénon map.^{2,3} At present, despite the immense literature available, it seems fair to say that shadowability is still a subject where problems vastly outnumber significant results.

The purpose of this paper is, first, to describe a simple numerical experiment profiting from the fact that the Hénon map has a unique inverse. As it is typical for any map having a unique inverse, one can in principle iterate the map forward any number of times and, using the inverse, return to the original point of departure. Here, we check how this “there and back” excursion fares numerically. Generically, dynamical systems with unique inverse provide a wide class of models to study round-off and propagation errors numerically using simple examples. Second, we provide a survey of some recent results and examples of a general methodology to obtain exact expressions for periodic orbits of the quadratic map in the partition generating limit, as well as the coordinates of their orbital points. Knowledge of the precise location of orbital points is a mean of obtaining exact markers, reference points in phase space, that help to quantify the impact of unavoidable round-off and noise errors that parasitize numerical solutions of equations of motion. Curiously, while the literature on shadowability is already immense, apparently in all this literature there are no explicit discussions of the impact of shadowability on real-life applications. Of course, as for Lorenz’s butterfly effect, it is not difficult to grasp the *conceptual* interest in shadowability. But an example of a practical situation where shadowability really makes a detectable difference seems to be still missing.

Before proceeding, we draw attention to the notion of *noninvertible* map. It is common to say that a dynamical system is noninvertible if the backward time evolution is either undefined or multivalued. In the present paper, the term *unique inverse* is used to clearly indicate situations where no branch ambiguity arises when taking the inverse. Of course, in general the number of inverses can vary from point to point or be undefined. Systems with multivalued inverse pose no intrinsic difficulty, just much more labor.

Table 1. Differences observed in the arrival distance from an arbitrarily selected initial point $(x_0, y_0) = (0.2, 0.7)$, after performing n forward followed by n inverse iterates of the Hénon map. The topmost set of data was obtained with 10 digits arithmetics, the middle set with 15 digits, and the bottom set with 30 digits. Here, $(a, b) = (1.4, 0.3)$. Manifestly, the huge distances shown have no practical use, but are just indicative of the numerical capabilities of the computer algebra system used.

Iterate	x	y	Distance from departure point
5	0.2000000000	0.7000000000	0
10	0.2014125000	0.7023640733	0.2753×10^{-2}
15	-2.801580008	25.58914483	25.06948
20	0.2120×10^{24}	0.1498×10^{42}	0.1498315×10^{42}
25	0.4649×10^{604}	0.7205×10^{1208}	0.7205×10^{1208}
30	0.1048×10^{75725}	$0.3663 \times 10^{151449}$	$0.3663 \times 10^{151449}$
5	0.2000000000000000	0.7000000000000000	0
10	0.200000005703233	0.700000009518633	0.1109×10^{-7}
15	0.200018165229800	0.700030318666333	0.3534×10^{-4}
20	0.0815040284379333	0.548873019665267	0.1920
25	873.988260542437	2546234.16352894	2546233.61
30	0.2165×10^{574}	0.1563×10^{1148}	0.1563×10^{1148}
5	0.2000000000000000	0.7000000000000000	0.
10	0.2000000000000000	0.7000000000000000	0.1028×10^{-22}
15	0.2000000000000000	0.7000000000000000	0.1162×10^{-19}
20	0.1999999999999999	0.6999999999999999	0.3407×10^{-15}
25	0.200000000001711	0.700000000002855	0.3329×10^{-11}
30	0.199999988783928	0.699999981280499	0.2182×10^{-7}

2. The there-and-back game with the Hénon map

As mentioned, maps with a unique inverse are good examples to learn about difficulties and round-off errors in numerically computed orbits.

Consider a standard textbook-example of a map with a unique inverse, the Hénon map⁴⁻⁶

$$\tilde{x} = a - x^2 + by, \quad (1)$$

$$\tilde{y} = x. \quad (2)$$

When $b \neq 0$, the unique inverse is

$$x = \tilde{y}, \quad (3)$$

$$y = (\tilde{x} - a + \tilde{y}^2)/b. \quad (4)$$

Clearly, the inverse means that, at least formally, one can forward iterate the map any arbitrary number of times and, from there, precisely return to the initial point of departure. But, does this also hold for numerical work? If not, after how many forward iterates can one return within a

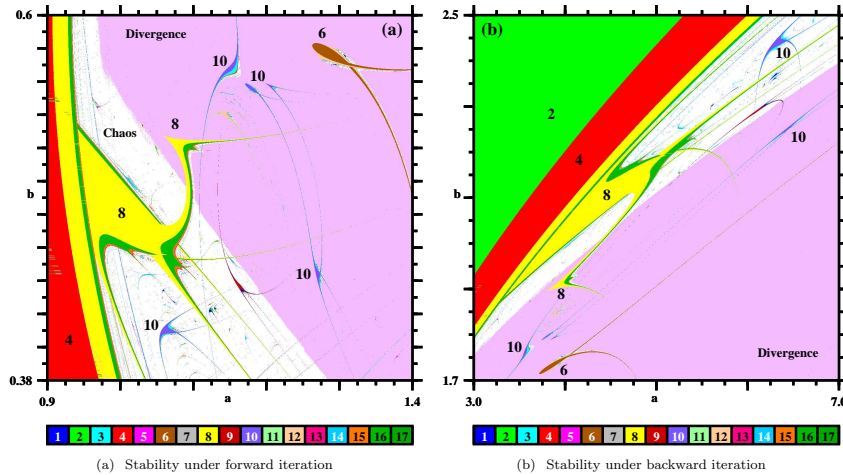


Fig. 1. The future and the past: Topological similarity between shape and distribution of stability phases in the control parameter space of (a) the Hénon map, and (b) the inverse Hénon map. Colors/shadings denote periods mod 17, as defined by the colorbar. White denotes chaos. Numbers represent the period of the main domains of major islands and are added to facilitate visual comparisons. Divergent (unbounded) orbits constitute roughly half of both windows. Resolution of each panel: 1200×1200 parameter points.

prescribed radius of the initial point? In other words, how far can we move from the initial point and safely come back? To investigate this question we use *Maple*, a computer algebra software which allows fixing the number of significant digits in computations with real numbers.

Table 1 illustrates typical results obtained when iterating the Hénon map forward and backward 30 times while fixing number of digits in the computations. As parameters, we select Hénon's classical values $(a, b) = (1.4, 0.3)$, and as initial point in phase space, we arbitrarily chose the point $(x_0, y_0) = (0.2, 0.7)$. This point lies relatively close to the chaotic attractor. To reduce the table size, iterates are recorded *modulo 5*. The top set of data in Table 1 was obtained with 10 digits arithmetics, the middle set with 15 digits, and the bottom set with 30 digits.

As seen from Table 1, moving five iterates forward and then backward always allow one to safely return to the original departure point, independently of using 10, 15 or 30 digits arithmetic. However, the situation starts to change considerably after moving 10 iterates forth and back. Ten iterates are barely able to bring one back to the point of departure with 10 digits arithmetics. Double precision computations normally use 15-16

digits and, therefore, allow safe excursions of about 10 iterates. However, 15 digits arithmetics fails spectacularly after some 20 iterates or so. Even when using 30 digits, which require the ability of performing arithmetic with dedicated software, do not allow very far excursions. One may suspect the divisions by b in Eq. (4) to cause loss of precision. By performing similar experiments with $b = \pm 1$ it is not difficult to realize this not to be the case.

Out of curiosity, we decided to compare the distribution of stability regions between the direct Hénon map, Eqs. (1)-(2), and the corresponding inverse map, Eqs. (3)-(4). To this end, phase diagrams were computed in the control parameter space as described in the literature.^{7,8} Figure 1 illustrates the results obtained for representative parameter windows. As seen from this figure, the formal similarity of both maps is reflected in the relatively isomorphic distribution of the stability phases, despite the strong shear present in Fig. 1(b) and the fact the window lies well outside the familiar stripe $-1 \leq b \leq 1$ typical of forward iteration of the Hénon map.⁷ Thus, to iterate forward or backward in time a map which has a unique inverse seems to produce quite similar distribution of stable periodic motions.

Before moving on, it is interesting to observe that, with the possible exception of the weak interaction,⁹ all known laws of physics do not distinguish between future and past, although observed phenomena are irreversible. It is an important and difficult open problem to find a theoretical explanation for the observed asymmetry in the direction of time, *time's arrow* in the words of Eddington.¹⁰

3. Exact coordinates of orbital points

Now, we consider the determination of exact orbital points in the so-called $a = 2$ *partition generating limit*⁴⁻⁶ of the quadratic or, equivalently, logistic map

$$x_{t+1} \equiv f(x_t) = a - x_t^2, \quad t = 0, 1, 2, \dots \quad (5)$$

For systems like this, with algebraic equations of motion, it is possible to use the standard *elementary symmetric functions*¹¹ to express individual periodic orbits as functions of the orbital points, which are roots of the periodic orbits. Using the so-called *Vieta's formulas*, the elementary symmetric functions may be expressed in a general manner by means of the coefficients of the orbital equation of motion, without the equation itself

being solved. Of particular interest in the present context is an observation by John Wallis (1616-1703), in *De Tractatus Algebra, Historicus et Practicus*, that “the coefficient of the second term [of any polynomial], reckoning downward from the highest, is the aggregate of all the roots...”

Accordingly, a fruitful quantity to express individual orbits of polynomial dynamical systems is the scalar which represents the sum σ of the orbital points. With σ , all possible orbits can be extracted from a single σ -parameterized polynomial $\psi_k(x)$, called the *orbital carrier*.^{12,13} For each period k , the corresponding values of the scalar σ are obtained as roots of an auxiliary polynomial $\mathbb{S}_k(\sigma)$, whose degree informs the total number of k -periodic orbits that exist in the system. As it is not difficult to realize, the study of the polynomial doublets $\psi_k(x)$ and $\mathbb{S}_k(\sigma)$ shifts the traditional study of *numerically approximate orbital points* to a new level, namely to the study of σ -parameterized *algebraically exact equations of motion*. Every periodic orbit can be parameterized by the sum σ of orbital points, and the method to do it is effective.¹³

A few examples help to understand what this is all about, and how it works. Consider the polynomial doublets $\psi_k(x)$ and $\mathbb{S}_k(\sigma)$ which encode all possible orbits of periods 4, 5 and 6 in the partition generating limit of the quadratic map. Explicitly, for period four the doublet is¹³

$$\begin{aligned} \psi_4(x) = & x^4 - \sigma x^3 + \frac{1}{2}(\sigma^2 + \sigma - 8)x^2 - \frac{1}{6}(\sigma^3 + 3\sigma^2 - 20\sigma + 2)x \\ & + \frac{1}{24}(\sigma - 3)(\sigma^3 + 9\sigma^2 - 2\sigma - 16) \end{aligned} \quad (6)$$

$$\mathbb{S}_4(\sigma) = (\sigma + 1)(\sigma^2 - \sigma - 4). \quad (7)$$

The degree of $\mathbb{S}_4(\sigma)$ tells us that there are three period-four orbits, one with integer coefficients and two with quadratic numbers as coefficients.

For period five the analogous doublet encoding all possible orbits is

$$\begin{aligned} \psi_5(x) = & (360\sigma^2 - 360\sigma - 240)x^5 - 120\sigma(3\sigma^2 - 3\sigma - 2)x^4 \\ & + 60(\sigma^2 + \sigma - 10)(3\sigma^2 - 3\sigma - 2)x^3 \\ & - (60\sigma^5 + 90\sigma^4 - 1800\sigma^3 + 1710\sigma^2 + 1860\sigma - 1200)x^2 \\ & + (15\sigma^6 + 45\sigma^5 - 735\sigma^4 + 375\sigma^3 + 3480\sigma^2 - 2700\sigma - 1200)x \\ & - 3\sigma^7 - 12\sigma^6 + 192\sigma^5 + 30\sigma^4 - 2061\sigma^3 + 1446\sigma^2 + 4248\sigma - 3600, \end{aligned} \quad (8)$$

$$\mathbb{S}_5(\sigma) = (\sigma - 1)(\sigma^2 + \sigma - 8)(\sigma^3 - \sigma^2 - 10\sigma + 8). \quad (9)$$

The total number of period-five orbits is six, the degree of $\mathbb{S}_5(\sigma)$. The orbit corresponding to the choice $\sigma = 1$ has integer coefficients, two orbits have quadratic numbers as coefficients, and three orbits have coefficients given by algebraic numbers of degree three.

Abbreviating $\varphi \equiv 3\sigma^3 - 7\sigma^2 - 13\sigma + 13$, for period six the doublet encoding

all possible orbits is

$$\begin{aligned} \psi_6(x) = & 160\varphi^2\sigma^2(x^6 - \sigma x^5) + 80\sigma^2(\sigma + 4)(\sigma - 3)\varphi^2x^4 \\ & - 40\sigma\varphi(2\sigma^7 + \sigma^6 - 86\sigma^5 + 126\sigma^4 + 358\sigma^3 - 343\sigma^2 - 50\sigma + 56)x^3 \\ & + 20\sigma^2\varphi(\sigma^7 + 3\sigma^6 - 70\sigma^5 + 48\sigma^4 + 679\sigma^3 - 683\sigma^2 - 1218\sigma + 1048)x^2 \\ & - 4\sigma\varphi(\sigma^9 + 6\sigma^8 - 91\sigma^7 - 78\sigma^6 + 1693\sigma^5 - 976\sigma^4 - 6911\sigma^3 + 5496\sigma^2 \\ & + 2508\sigma - 2128)x + 2\sigma^{14} + 14\sigma^{13} - 247\sigma^{12} - 268\sigma^{11} + 7984\sigma^{10} \\ & - 8072\sigma^9 - 80966\sigma^8 + 157668\sigma^7 + 184938\sigma^6 - 530694\sigma^5 \\ & + 88965\sigma^4 + 373032\sigma^3 - 197156\sigma^2 - 13440\sigma + 15680, \quad (10) \\ \mathbb{S}_6(\sigma) = & (\sigma + 1)(\sigma - 1)(\sigma^3 - 21\sigma + 28)(\sigma^4 + \sigma^3 - 24\sigma^2 - 4\sigma + 16). \quad (11) \end{aligned}$$

Now, the total number of orbits is nine, the degree of $\mathbb{S}_6(\sigma)$. Two orbits have integer coefficients, three have coefficients given by algebraic numbers of degree three, and four have coefficients given by algebraic numbers of degree four. All these exact informations regarding the algebraic nature of the orbits are not possible to extract from numerical approximations of the orbital equations of motion, independently of the number of digits used for their computation.

As mentioned, when substituted into $\psi_k(x)$, each individual root of $\mathbb{S}_k(\sigma) = 0$ “projects” $\psi_k(x)$ into the specific orbital equation corresponding to σ . Normally, the polynomials $\mathbb{S}_k(\sigma)$ factor over the integers: factors with degree $\partial_k > 1$ correspond to orbital *clusters*, namely to irreducible polynomial aggregates commingling together a total of ∂_k orbits. Linear factors, multiple or not, correspond to non-clustered *single* orbits of period k . For instance, substituting $\sigma = -1$ into $\psi_4(x)$ we obtain the non-clustered orbit $o_{4,1}(x)$, while for $\sigma = (1 - \sqrt{17})/2$ and $\sigma = (1 + \sqrt{17})/2$, roots of the quadratic factor in $\mathbb{S}_4(\sigma)$, we get the orbits $o_{4,2}(x)$ and $o_{4,3}(x)$, respectively:

$$o_{4,1}(x) = x^4 + x^3 - 4x^2 - 4x + 1, \quad (12)$$

$$o_{4,2}(x) = x^4 - \frac{1}{2}(1 - \sqrt{17})x^3 - \frac{1}{2}(3 + \sqrt{17})x^2 - (2 + \sqrt{17})x - 1, \quad (13)$$

$$o_{4,3}(x) = x^4 - \frac{1}{2}(1 + \sqrt{17})x^3 - \frac{1}{2}(3 - \sqrt{17})x^2 - (2 - \sqrt{17})x - 1. \quad (14)$$

Note that the last two orbits have more complicated algebraic coefficients enforced by the σ values underlying them. When multiplied together, $o_{4,2}(x)$ and $o_{4,3}(x)$ produce an orbital cluster, or aggregate:

$$\begin{aligned} c_{4,1}(x) &= o_{4,2}(x) \times o_{4,3}(x) \\ &= x^8 - x^7 - 7x^6 + 6x^5 + 15x^4 - 10x^3 - 10x^2 + 4x + 1, \quad (15) \end{aligned}$$

a cluster obtainable directly by eliminating σ between $\psi_4(x)$ and $\sigma^2 - \sigma - 4$.

Note that the product of $o_{4,2}(x)$ and $o_{4,3}(x)$, which individually have algebraic coefficients, resulted in a cluster with integer coefficients, a generic characteristic of conjugated orbits with algebraic coefficients. Technically, $o_{4,2}(x)$ and $o_{4,3}(x)$ are defined by *relative*¹⁴ quartic equations of motion, because their coefficients are algebraic numbers, not integers. Manifestly, $c_{4,1}(x)$ decomposes over the field $\mathbb{Q}(\sqrt{17})$. Furthermore, note that $o_{4,1}(x)$ provides an exact representation of the

orbit and has simple integer coefficients. In sharp contrast, the numerical representation of $o_{4,2}(x)$ and $o_{4,3}(x)$ will have necessarily approximate numerical coefficients. Thus, the symmetries that are clearly visible between Eqs. (13) and (14) are totally obliterated when considering numerically approximated “projections” of the orbits. This unambiguous dichotomic distinction between algebraically exact and numerically approximate orbits remains valid for other periods and displays clearly the powerful insight obtained by working with exact equations of motion.

Doublets like Eqs. (6)-(7), (8)-(9), and (10)-(11) may be determined systematically, in principle for any arbitrary period. Doublets for arbitrary values of a of the quadratic map and arbitrary (a, b) of the Hénon map are available.^{15,16}

Similarly, eliminating σ between $\psi_5(x)$ and, successively, $\sigma - 1$, $\sigma^2 + \sigma - 8$, and $\sigma^3 - \sigma^2 - 10\sigma + 8$, we get, apart from multiplicative constants used to eliminate denominators in $\psi_5(x)$, the following orbits and orbital clusters:

$$\begin{aligned} o_{5,1}(x) &= x^5 - x^4 - 4x^3 + 3x^2 + 3x - 1, \\ c_{5,1}(x) &= x^{10} + x^9 - 10x^8 - 10x^7 + 34x^6 + 34x^5 - 43x^4 \\ &\quad - 43x^3 + 12x^2 + 12x + 1, \\ c_{5,2}(x) &= x^{15} - x^{14} - 14x^{13} + 13x^{12} + 78x^{11} - 66x^{10} - 220x^9 + 165x^8 \\ &\quad + 330x^7 - 210x^6 - 252x^5 + 126x^4 + 84x^3 - 28x^2 - 8x + 1. \end{aligned}$$

The clusters factor into quintics over $\mathbb{Q}(\sqrt{33})$ and $\mathbb{Q}(\sqrt[3]{-62 + 95\sqrt{-3}})$, respectively, thereby providing explicit analytic expressions for the remaining five period-five orbits. Such clustered orbits involve relative¹⁴ quintic equations, namely quintics whose coefficients are algebraic numbers (not integers), and which cannot be represented exactly in numerical computations.

For period-six there are nine possible orbits encoded simultaneously by $\psi_6(x)$ and $\mathbb{S}_6(\sigma)$. Apart from multiplicative constants used to eliminate denominators in $\psi_6(x)$, by selecting $\sigma = 1$ and $\sigma = -1$ we get the orbits with real coefficients and discriminants $\Delta_{6,1}$ and $\Delta_{6,2}$:

$$\begin{aligned} o_{6,1}(x) &= x^6 - x^5 - 5x^4 + 4x^3 + 6x^2 - 3x - 1, & \Delta_{6,1} &= 371293 = 13^5, \\ o_{6,2}(x) &= x^6 + x^5 - 6x^4 - 6x^3 + 8x^2 + 8x + 1, & \Delta_{6,2} &= 453789 = 3^3 \cdot 7^5. \end{aligned}$$

It is interesting to observe that $o_{6,1}(x)$ and $o_{6,2}(x)$ imply a contrived twist in the current understanding of polynomial interdependence. Individually, they are obtained as two seemingly independent “projections” which, however, have the carrier $\psi_6(x)$ as their common origin. Therefore, rather than being *de facto* independent orbits, they are in a certain sense “conjugated” orbits. Furthermore, since all nine period-six orbits arise from the same carrier $\psi_6(x)$, the orbits $o_{6,1}(x)$ and $o_{6,2}(x)$ are also conjugated to all other seven orbits. This illustrates the existence of a complex and quite subtle *carrier-conjugation*, i.e. an arithmetical interdependence lurking among all period- k orbits, which is rather different from the field isomorphisms familiar from Galois theory of equations.²² For arbitrary periods k , the orbital carriers $\psi_k(x)$ allow all its carrier-conjugated orbits to

Table 2. The nine period-six orbits $o_{6,j}$ of the map $x_{t+1} = 2 - x_t^2$. Here, $\sigma_{6,j} = \sum x_j$ is the sum of the orbital points. The triad and quartet of $\sigma_{6,j}$ values are roots of the cubic and quartic factors in Eq. (11), respectively.

Orbit	x_1	$\sigma_{6,j}$
$o_{6,1}$	-1.770912051306	1
$o_{6,2}$	-1.911145611572	-1
$o_{6,3}$	-1.990061550730	-5.142457360
$o_{6,4}$	-1.756443146740	1.491252188
$o_{6,5}$	-0.912421314706	3.651205171
$o_{6,6}$	-1.990663269435	-5.287613777
$o_{6,7}$	-1.916491658218	-0.902246984
$o_{6,8}$	-1.559348708126	0.756484903
$o_{6,9}$	-0.971966826485	4.433375858

have coefficients belonging to very distinct number fields, a remarkable twist in the concept of conjugation which is not compatible with the standard canons of number field theory.

As before, for roots of the cubic and quartic factors in Eq. (11), the resulting coefficients in Eq. (10) are more complicated algebraic numbers, not integers. When all orbits arising from the same σ -factor are multiplied together one obtains a cluster, a polynomial aggregate with integer coefficients and degree $\partial = mk$, multiple of the period k , where $m > 1$ is an integer. For instance,

$$c_{6,1}(x) = x^{18} - 18x^{16} + x^{15} + 135x^{14} - 15x^{13} - 546x^{12} + 90x^{11} + 1287x^{10} - 276x^9 - 1782x^8 + 459x^7 + 1385x^6 - 405x^5 - 534x^4 + 170x^3 + 72x^2 - 24x + 1, \quad (16)$$

$$c_{6,2}(x) = x^{24} + x^{23} - 24x^{22} - 23x^{21} + 252x^{20} + 229x^{19} - 1521x^{18} - 1292x^{17} + 5832x^{16} + 4540x^{15} - 14822x^{14} - 10282x^{13} + 25284x^{12} + 15001x^{11} - 28667x^{10} - 13653x^9 + 20886x^8 + 7168x^7 - 9126x^6 - 1802x^5 + 2085x^4 + 101x^3 - 180x^2 + 12x + 1. \quad (17)$$

Table 2 collects numerical approximations for one orbital point for all nine period-six orbits, together with the corresponding sums $\sigma_{6,j}$. All other orbital points may be easily obtained from x_1 by iterating the map $x_{t+1} = 2 - x_t^2$.

As for the remaining polynomials, the orbit $o_{6,1}(x)$ factors into a pair of cubics over $\mathbb{Q}(\sqrt{13})$. The cluster $c_{6,2}(x)$ factors into two equations of degree nine over $\mathbb{Q}(\sqrt{21})$. However, such nine-degree polynomials mix roots of two distinct orbits, since their degree is not a multiple of six. For the cluster $c_{6,1}(x)$, the proper six cubics are obtained over $\mathbb{Q}(\sqrt[3]{\alpha})$, where $\alpha = -154 + 42\sqrt{-3} - 18\sqrt{-7} + 30\sqrt{21}$. For the cluster $c_{6,2}(x)$, eight cubics are obtained over $\mathbb{Q}(\sqrt{\beta})$, where $\beta = 65 - 13\sqrt{5} + 15\sqrt{15} - 3\sqrt{65}$. These factorizations provide explicit and exact solutions for all period-six orbits and their orbital points, which are roots of the cubics. Manifestly, the factors of $\mathbb{S}_k(\sigma)$ reveal how orbits are distributed into clusters and

Table 3. The eighteen period-seven orbits, characterized by one orbital point and the sum $\sigma_{7,j}$ of all points. The remaining orbital points follow by iterating $x_{t+1} = 2 - x_t^2$.

Orbit	x_1	$\sigma_{7,j}$
$o_{7,1}$	-1.9786867361502203955847071	-2.8882360088434114464952734
$o_{7,2}$	-1.8108964749862932314435851	-0.6150716258115650649303224
$o_{7,3}$	-1.0418806809758605723525628	4.5033076346549765114255959
$o_{7,4}$	-1.9976281104816460923503281	-7.2481321962698823504243586
$o_{7,5}$	-1.8848761656674288384473805	-1.2290602270284331761618286
$o_{7,6}$	-1.9409835883148106464466346	-0.77490800237038950156013044
$o_{7,7}$	-1.6122889835107255448466855	1.8441318528399982410921511
$o_{7,8}$	-1.7197459866836201484847537	2.7448245616149058389987627
$o_{7,9}$	-1.2029816300037407895687593	3.6631440112138009480554039
$o_{7,10}$	-1.9975528324285225652564052	-7.1754350638396879312221350
$o_{7,11}$	-1.9780114089762614447581210	-2.9359943127153307953060572
$o_{7,12}$	-1.8812582592076877545063517	-1.6023708208031626612700681
$o_{7,13}$	-1.9391197295964931429508120	-0.52557288374288388601167975
$o_{7,14}$	-1.8049930381548525612803578	0.019650748046206826205286560
$o_{7,15}$	-1.6004083969600341010740502	2.1979580475223842977306042
$o_{7,16}$	-1.7110701448170319282769643	2.3647347938971127665283378
$o_{7,17}$	-1.1795694263410389611326784	3.2907783266632442601391821
$o_{7,18}$	-1.0142477277395461818441842	5.3662511649721171232065293

single orbits, if any.

We remark that, while the derivation of the carriers $\psi_k(x)$ becomes increasingly more laborious as the period k grows, knowledge of approximate numerical values of the orbital points suffices to disclose exact expressions for the polynomials $\mathbb{S}_k(\sigma)$ and its factors, thereby revealing the algebraic character of all orbits encoded by the carriers.

For instance, although the exact analytic expression for $\psi_7(x)$ remains yet to be obtained, Table 3 displays data from which one easily finds exact expression and factors for $\mathbb{S}_7(\sigma) = s_3(\sigma)s_6(\sigma)s_{18}(\sigma)$, namely

$$\begin{aligned}
 s_3(\sigma) &= \prod_{j=1}^3 (\sigma - \sigma_{7,j}) = \sigma^3 - \sigma^2 - 14\sigma - 8, \\
 s_6(\sigma) &= \prod_{j=4}^9 (\sigma - \sigma_{7,j}) = \sigma^6 + \sigma^5 - 39\sigma^4 + 63\sigma^3 + 110\sigma^2 - 136\sigma - 128, \\
 s_9(\sigma) &= \prod_{j=10}^{18} (\sigma - \sigma_{7,j}) = \sigma^9 - \sigma^8 - 56\sigma^7 + 118\sigma^6 + 573\sigma^5 - 1249\sigma^4 \\
 &\quad - 1582\sigma^3 + 2700\sigma^2 + 1576\sigma - 32.
 \end{aligned}$$

As it is not difficult to recognize, analogously as before, the individual factors composing $\mathbb{S}_k(\sigma)$ reveal important informations about the number fields underlying conjugate orbits. For instance, $s_3(\sigma)$, $s_6(\sigma)$ and $s_{18}(\sigma)$ define the algebraic

nature of the number fields composing the conjugate clusters entangled in $\psi_7(x)$ which, in their turn, define all individual period-seven orbits as well as the algebraic nature of their orbital points. First, for period seven there are no orbits with integer coefficients. Second, there are three clusters defining period-seven orbits. Third, the orbits forming these three clusters are relative polynomials of degree seven, with coefficients defined by algebraic numbers of degrees 3, 6, and 18. These predictions should be validated as soon as $\psi_7(x)$ is explicitly determined. Manifestly, similar predictions may be obtained for all periods $k > 7$. There are 30 period-8 orbits, 56 of period nine, 99 of period ten, and so on.^{17,18} Explicit expressions for $\mathbb{S}_8(\sigma)$, $\mathbb{S}_9(\sigma)$, $\mathbb{S}_{10}(\sigma)$, as well as their composing factors, are already available.¹⁹

4. Orbital inheritance: solving high degree equations

Another possibility to obtain exact analytical representation for periodic orbital points, that may act as reference points to investigate numerical errors, is to use “inherited” orbits.^{13,19–21} A simple example allows one to grasp easily what inheritance means. To this end, consider the nonlinear transformation $x^3 - 3x$ applied to $o_{6,2}(x)$, namely¹³

$$c_{6,1}(x) = o_{6,2}(x^3 - 3x). \quad (18)$$

This identity shows that, as soon as the roots z_i of the orbit $o_{6,2}(x)$ are determined analytically in an exact manner, namely

$$o_{6,2}(x) = \left(x^3 + \frac{1}{2}(1 - \sqrt{21})x^2 - \frac{1}{2}(1 + \sqrt{21})x + \frac{1}{2}(5 + \sqrt{21}) \right) \times \\ \left(x^3 + \frac{1}{2}(1 + \sqrt{21})x^2 - \frac{1}{2}(1 - \sqrt{21})x + \frac{1}{2}(5 - \sqrt{21}) \right), \quad (19)$$

three new orbits follow from them by solving the six cubics

$$x^3 - 3x - z_i = 0, \quad i = 1, 2, \dots, 6, \quad (20)$$

which, obviously, may be also determined exactly. Thus, these eighteen roots provide exact analytical representations in terms of radicals for all orbital points composing the 18th-degree cluster $c_{6,1}(x)$ of Eq. (16). We remark that exact explicit solutions for non-trivial polynomials of degrees five and higher are increasingly more difficult and rare to find.²² In particular, we are not aware of any previous explicit exact solution of a degree-eighteen polynomial.

Analogous results concerning orbital inheritance for periods $k \leq 12$ are available in the literature.¹³

5. Preperiodic points as access to exact orbital points

In the partition generating limit it is easy to obtain preperiodic points which, when used as initial conditions to iterate the map $x_{t+1} = 2 - x_t^2$, grant access to the exact coordinates of orbital points of periodic orbits.¹⁹ Such useful preperiodic

points are roots of an infinite family of polynomials $Q_\ell(x)$, which may be easily generated by a recurrence relation, Eq. (21) below. These preperiodic points were previously used¹⁹ to extract specific orbital equations embedded in polynomial clusters with degree exceeding one billion and, therefore, totally out of reach by ordinary brute-force polynomial factorization. But we now find that preperiodic points can be also used to generate systematically, one by one, *explicit coordinates of periodic points for all orbits* of the quadratic map, Eq. (5).

The $Q_\ell(x)$ polynomials are obtained as irreducible factors composing an auxiliary family of polynomials, $T_\ell(x)$, generated recursively. Starting from two given initial *seed functions*, $T_0(x)$ and $T_1(x)$, all subsequent auxiliary $T_\ell(x)$ are obtained from the recurrence²³

$$T_\ell(x) = xT_{\ell-1}(x) - T_{\ell-2}(x), \quad \ell = 2, 3, 4, \dots \quad (21)$$

For our present purpose, we fix $T_0(x) = 2$ and $T_1(x) = x$. Instead of the above recurrence, one may also obtain $T_\ell(x)$ directly, with no need of knowing every $T_{\ell'}(x)$ with $\ell' < \ell$, using Pincherle's relation²⁴

$$T_\ell(x) = \left(\frac{x - \sqrt{x^2 - 4}}{2} \right)^\ell + \left(\frac{x + \sqrt{x^2 - 4}}{2} \right)^\ell, \quad \ell = 0, 1, 2, \dots \quad (22)$$

Clearly, $T_1(x) = Q_1(x) = x$, and $T_2(x) = Q_2(x) = x^2 - 2$. For $\ell > 2$, the polynomials $T_\ell(x)$ are reducible over the integers, products of *cyclotomic-like* irreducible factors $Q_\ell(x)$, except for $\ell = 2^n$, $n = 1, 2, 3, \dots$ when $T_\ell(x) = Q_\ell(x)$, which are irreducible. Every new $T_\ell(x)$ generated by Eq. (21) contributes a new irreducible factor $Q_\ell(x)$, new in the sense of not appearing for any index ℓ' smaller than ℓ . Thus, the next first few polynomials are

$$\begin{aligned} T_3(x) &= Q_1(x)Q_3(x), & T_4(x) &= Q_4(x), & T_5(x) &= Q_1(x)Q_5(x), \\ T_6(x) &= Q_2(x)Q_6(x), & T_7(x) &= Q_1(x)Q_7(x), & T_8(x) &= Q_8(x), \end{aligned}$$

where

$$\begin{aligned} Q_3(x) &= x^2 - 3, & Q_4(x) &= x^4 - 4x^2 + 2, & Q_5(x) &= x^4 - 5x^2 + 5, \\ Q_6(x) &= x^4 - 4x^2 + 1, & Q_7(x) &= x^6 - 7x^4 + 14x^2 - 7, \end{aligned}$$

and $Q_8(x) = x^8 - 8x^6 + 20x^4 - 16x^2 + 2$. The first twenty $Q_\ell(x)$ are listed in Table 1 of an open access paper¹⁹ while the first 100 $Q_\ell(x)$ are shown in Table A.1 in the Appendix below. A key observation is that the *irreducible* $Q_\ell(x)$ are the building blocks of the *reducible* auxiliary $T_\ell(x)$. Using the roots of $Q_\ell(x)$ as starting conditions to iterate the quadratic map, Eq. (5), one finds that after a finite preperiodic start, i.e. a certain number of non-repeating iterates, the iteration lands on a cycle of k distinct points that repeats forever.

6. Conclusions and outlook

We are used to think that the most common classes of models of dynamical systems involve either *discrete-time* maps or *continuous-time* differential equations. This simplistic separation ignores the fact that, when it comes to find *explicit solutions* for equations of motion, apart from a measure-zero set of equations discussed in textbooks of calculus and dynamics, the solution of differential equations are normally obtained after representing the differential equations by approximate time-discrete maps which, unfortunately, depend on the integration step or steps of the specific procedure adopted. Thus, to find explicit solutions of differential equations means to artfully select a range for the integration step where solutions remain stable in the sense that they do not change *significantly* under slight changes of the integration step. As it is known, the finiteness of the integration step is an unavoidable source of error in the numerical solution of differential equations. Even in rare cases when formulas for error estimates are available, such estimates are virtually never addressed in real-life applications. In sharp contrast, maps can yield the “correct” temporal evolution free from the aforementioned errors of numerical methods, provided that the maps faithfully represent the dynamics, and that calculations are performed under strict control of the numerical precision. Thus, in one way or another, modulo a measure-zero set of analytically solvable problems, to find explicit solutions for equations of motion means, in fact, to iterate maps or, equivalently, to assume that the *dynamics is inevitably governed by discrete-time variables*.

For the large class of maps with unique inverse, we believe the there-and-back game summarized in Table 1 to provide a viable tool to gauge numerical precision of calculations. For the complementary class of systems with multiple inverses the there-and-back game should of course be still possible, albeit much more complicated to implement. We argued that one should seek exact analytical solutions of simple problems and use them as reference marks in phase-space to test if numerical work is being done with enough precision. Of course, in general we will still remain in the dark as usual, having to resort to the standard rules of thumb. Be it as it may, we believe that physical systems with unique inverses should be explored under the new light discussed here, in particular to understand the interconnections between stability diagrams like the ones in Fig. 1.

From a theoretical point of view, we argued that orbital carriers, imply the startling and subtle notion of carrier-conjugates i.e. an unexpected arithmetical interdependence lurking among all period- k orbits, which is distinct from the familiar field isomorphisms from Galois theory of equations. For any arbitrary period k , the orbital carrier $\psi_k(x)$ allow all its carrier conjugated orbits to have coefficients belonging to very distinct number fields, a remarkable twist in the concept of conjugation, not compatible with the standard canons of number field theory. Orbital carriers certainly exist for any dynamical system governed by algebraic equations of motion, a wide class of systems, although it may not be feasible to obtain them explicitly for arbitrary systems. Fortunately, as illustrated above, the quadratic map of Eq. (5) allows one to explore carriers explicitly.

Acknowledgments

This work was started during a visit to the Max-Planck Institute for the Physics of Complex Systems, Dresden, gratefully supported by an Advanced Study Group on *Forecasting with Lyapunov vectors*. The author was partially supported by CNPq, Brazil, grant 304719/2015-3.

A.1. Appendix

Table A.1 lists the first 100 irreducible polynomials $Q_\ell(x)$ as factors of the corresponding $T_\ell(x)$. Manifestly, the *irreducible* $Q_\ell(x)$ are the building blocks of the *reducible* auxiliary $T_\ell(x)$. The polynomials $Q_\ell(x)$ divide themselves naturally into two groups, according to the odd or even character of ℓ . Further, $Q_1(x) = x$ is a factor of $T_\ell(x)$ for odd values of ℓ , while $Q_{2^\ell}(x)$ is a factor of $T_{2^\ell}(x)$, for $\ell = 1, 2, 3, \dots$. Additionally, the power $p \equiv 2^\ell$ divides the indices of all factors composing $T_p(x)$.

The regularity observed in Table A.1 between the base factors of ℓ and the subindexes of $Q_\ell(x)$ reveals how to generate the decomposition indices of $T_\ell(x)$ automatically. For example, for odd values of $\ell = b_1^{p_1} b_2^{p_2}$ the following Maple driver generates the list of $Q_\ell(x)$ indices which appear in the factorization $T_\ell(x)$:

```
with(ListTools):
b1 := 3:    b2 := 5:
p1 := 3:    p2 := 2:    L := [NULL]:
for ijk from 0 to p1 do
for lmn from 0 to p2 do
    aux:= b1^ijk * b2^lmn:
    L := [op(L),aux]:    od: od:
print( b1^p1 * b2^p2, sort(MakeUnique(L)) );
```

This driver may be easily adapted to deal with more complicated values of ℓ . For higher odd values of ℓ we determined explicitly the decompositions:

$$\begin{aligned} 225 = 3^2 5^2 : & \quad T_{225} = Q_1 Q_3 Q_5 Q_9 Q_{15} Q_{25} Q_{45} Q_{75} Q_{225}, \\ 441 = 3^2 7^2 : & \quad T_{441} = Q_1 Q_3 Q_7 Q_9 Q_{21} Q_{49} Q_{63} Q_{147} Q_{441}. \end{aligned}$$

However, for $675 = 3^3 \cdot 5^2$ the software and hardware available to us could not generate $T_{675}(x)$. The driver above was then used to obtain the following illustrative lists of decomposition indices:

$$\begin{aligned} 675 = 3^3 5^2 : & \quad [1, 3, 5, 9, 15, 25, 27, 45, 75, 135, 225, 675] \\ 729 = 3^2 9^2 : & \quad [1, 3, 9, 27, 81, 243, 729] \\ 1089 = 3^2 11^2 : & \quad [1, 3, 9, 11, 33, 99, 121, 363, 1089] \end{aligned}$$

Table A.1 leads us to conjecture an interesting theoretical possibility about the $Q_\ell(x)$ polynomials, which share remarkable similarities with the *cyclotomic*

Table A.1. The first 100 factors $Q_\ell(x)$ of $T_\ell(x)$.

i Odd			i Even		
ℓ	Factors	$T_\ell(x)$	ℓ	Factors	$T_\ell(x)$
1	1	Q_1	2	2	Q_2
3	3	Q_1Q_3	4	2^2	Q_4
5	5	Q_1Q_5	6	$2 \cdot 3$	Q_2Q_6
7	7	Q_1Q_7	8	2^3	Q_8
9	3^2	$Q_1Q_3Q_9$	10	$2 \cdot 5$	Q_2Q_{10}
11	11	Q_1Q_{11}	12	$2^2 \cdot 3$	Q_4Q_{12}
13	13	Q_1Q_{13}	14	$2 \cdot 7$	Q_2Q_{14}
15	$3 \cdot 5$	$Q_1Q_3Q_5Q_{15}$	16	2^4	Q_{16}
17	17	Q_1Q_{17}	18	$2 \cdot 3^2$	$Q_2Q_6Q_{18}$
19	19	Q_1Q_{19}	20	$2^2 \cdot 5$	Q_4Q_{20}
21	$3 \cdot 7$	$Q_1Q_3Q_7Q_{21}$	22	$2 \cdot 11$	Q_2Q_{22}
23	23	Q_1Q_{23}	24	$2^3 \cdot 3$	Q_8Q_{24}
25	5^2	$Q_1Q_5Q_{25}$	26	$2 \cdot 13$	Q_2Q_{26}
27	3^3	$Q_1Q_3Q_9Q_{27}$	28	$2^2 \cdot 7$	Q_4Q_{28}
29	29	Q_1Q_{29}	30	$2 \cdot 3 \cdot 5$	$Q_2Q_6Q_{10}Q_{30}$
31	31	Q_1Q_{31}	32	2^5	Q_{32}
33	$3 \cdot 11$	$Q_1Q_3Q_{11}Q_{33}$	34	$2 \cdot 17$	Q_2Q_{34}
35	$5 \cdot 7$	$Q_1Q_5Q_7Q_{35}$	36	$2^2 \cdot 3^2$	$Q_4Q_{12}Q_{36}$
37	37	Q_1Q_{37}	38	$2 \cdot 19$	Q_2Q_{38}
39	$3 \cdot 13$	$Q_1Q_3Q_{13}Q_{39}$	40	$2^3 \cdot 5$	Q_8Q_{40}
41	41	Q_1Q_{41}	42	$2 \cdot 3 \cdot 7$	$Q_2Q_6Q_{14}Q_{42}$
43	43	Q_1Q_{43}	44	$2^2 \cdot 11$	Q_4Q_{44}
45	$3^2 \cdot 5$	$Q_1Q_3Q_5Q_9Q_{15}Q_{45}$	46	$2 \cdot 23$	Q_2Q_{46}
47	47	Q_1Q_{47}	48	$2^4 \cdot 3$	$Q_{16}Q_{48}$
49	7^2	$Q_1Q_7Q_{49}$	50	$2 \cdot 5^2$	$Q_2Q_{10}Q_{50}$
51	$3 \cdot 17$	$Q_1Q_3Q_{17}Q_{51}$	52	$2^2 \cdot 13$	Q_4Q_{52}
53	53	Q_1Q_{53}	54	$2 \cdot 3^3$	$Q_2Q_6Q_{18}Q_{54}$
55	$5 \cdot 11$	$Q_1Q_5Q_{11}Q_{55}$	56	$2^3 \cdot 7$	Q_8Q_{56}
57	$3 \cdot 19$	$Q_1Q_3Q_{19}Q_{57}$	58	$2 \cdot 29$	Q_2Q_{58}
59	59	Q_1Q_{59}	60	$2^2 \cdot 3 \cdot 5$	$Q_4Q_{12}Q_{20}Q_{60}$
61	61	Q_1Q_{61}	62	$2 \cdot 31$	Q_2Q_{62}
63	$3^2 \cdot 7$	$Q_1Q_3Q_7Q_9Q_{21}Q_{63}$	64	2^6	Q_{64}
65	$5 \cdot 13$	$Q_1Q_5Q_{13}Q_{65}$	66	$2 \cdot 3 \cdot 11$	$Q_2Q_6Q_{22}Q_{66}$
67	67	Q_1Q_{67}	68	$2^2 \cdot 17$	Q_4Q_{68}
69	$3 \cdot 23$	$Q_1Q_3Q_{23}Q_{69}$	70	$2 \cdot 5 \cdot 7$	$Q_2Q_{10}Q_{14}Q_{70}$
71	71	Q_1Q_{71}	72	$2^3 \cdot 3^2$	$Q_8Q_{24}Q_{72}$
73	73	Q_1Q_{73}	74	$2 \cdot 37$	Q_2Q_{74}
75	$3 \cdot 5^2$	$Q_1Q_3Q_5Q_{15}Q_{25}Q_{75}$	76	$2^2 \cdot 19$	Q_4Q_{76}
77	$7 \cdot 11$	$Q_1Q_7Q_{11}Q_{77}$	78	$2 \cdot 3 \cdot 13$	$Q_2Q_6Q_{26}Q_{78}$
79	79	Q_1Q_{79}	80	$2^4 \cdot 5$	$Q_{16}Q_{80}$
81	3^4	$Q_1Q_3Q_9Q_{27}Q_{81}$	82	$2 \cdot 41$	Q_2Q_{82}
83	83	Q_1Q_{83}	84	$2^2 \cdot 3 \cdot 7$	$Q_4Q_{12}Q_{28}Q_{84}$
85	$5 \cdot 17$	$Q_1Q_5Q_{17}Q_{85}$	86	$2 \cdot 43$	Q_2Q_{86}
87	$3 \cdot 29$	$Q_1Q_3Q_{29}Q_{87}$	88	$2^3 \cdot 11$	Q_8Q_{88}
89	89	Q_1Q_{89}	90	$2 \cdot 3^2 \cdot 5$	$Q_2Q_6Q_{10}Q_{18}Q_{30}Q_{90}$
91	$7 \cdot 13$	$Q_1Q_7Q_{13}Q_{91}$	92	$2^2 \cdot 23$	Q_4Q_{92}
93	$3 \cdot 31$	$Q_1Q_3Q_{31}Q_{93}$	94	$2 \cdot 47$	Q_2Q_{94}
95	$5 \cdot 19$	$Q_1Q_5Q_{19}Q_{95}$	96	$2^5 \cdot 3$	$Q_{32}Q_{96}$
97	97	Q_1Q_{97}	98	$2 \cdot 7^2$	$Q_2Q_{14}Q_{98}$
99	$3^2 \cdot 11$	$Q_1Q_3Q_9Q_{11}Q_{33}Q_{99}$	100	$2^2 \cdot 5^2$	$Q_4Q_{20}Q_{100}$

polynomials²⁵ which may be generated by the quadratic map for $a = 0$. As it is known, every cyclotomic field is an Abelian extension of the rational numbers \mathbb{Q} . In this context, an important discovery is the so-called Kronecker-Weber theorem, stating that every finite Abelian extension of \mathbb{Q} can be generated by roots of unity, i.e. Abelian extensions are contained within some cyclotomic field.

In other words, every algebraic integer whose Galois group is Abelian can be expressed as a sum of roots of unity with rational coefficients. For details see, e.g., Edwards.²⁶ The study of the partition generating limit of the quadratic map $x_{t+1} = a - x_t^2$ seems to lend hope that for $a = 2$ the map may also share an analogous correspondence with Abelian equations as the one embodied in the Kronecker-Weber theorem²⁷ when $a = 0$. The dynamics for other values of a , when real and complex orbits coexist, is totally open to investigation. Integer and rational values of a are first good candidates to learn how bifurcation cascades unfold arithmetically. In particular the case $a = 1$, say, offers the possibility of learning about the interplay of infinite cascades of coexisting orbits governed by towers of real and complex algebraic quantities, a new and totally unexplored world. The investigation of these problems will certainly provide useful insight regarding the intricate algebraic nested induced by the dynamics. Clearly, these open problems deserve to be investigated.

References

1. K. Palmer, *Shadowing in Dynamical Systems, Theory and Applications*, (Springer, Dordrecht, 2000).
2. A. Carvalho, M. Lyubich, and M. Martens, *Renormalization in the Hénon family, I: Universality but non-rigidity*, 2005. Available at <https://arxiv.org/pdf/math/0508477.pdf>
3. M. Lyubich, and M. Martens, *Renormalization in the Hénon family, II: The heteroclinic web*, 2008. Available at <https://arxiv.org/pdf/0804.0780.pdf>
4. J. Argyris, G. Faust, M. Haase, and R. Friedrich, *An Exploration of Dynamical Systems and Chaos, Second Edition* (Springer, Berlin, 2015).
5. S. Strogatz, *Nonlinear Dynamics and Chaos, 2nd Edition* (CRC Press, Boca Raton, 2015)
6. M. Cencini, F. Cecconi, and A. Vulpiani, *Chaos - From Simple Models to Complex Systems* (World Scientific, Singapore, 2010).
7. J.A.C. Gallas, Structure of the parameter space of the Hénon map, *Phys. Rev. Lett.* **70**, 2714-2717 (1993).
8. R.E. Francke, T. Pöschel, and J.A.C. Gallas, Zig-zag networks of self-excited periodic oscillations in a tunnel diode and a fiber-ring laser, *Phys. Rev. E* **87**, 042907 (2013).
9. J.P. Lees et al. (The BABAR Collaboration) Observation of time-reversal violation in the B^0 meson system, *Phys. Rev. Lett.* **109**, 211801 (2012).
10. A.S. Eddington, *The Nature of the Physical World* (Macmillan, London, 1928).
11. H.G. Funkhouser, A short account of the history of symmetric functions of roots of equations, *Amer. Math. Monthly* **37**, 357-365 (1930).
12. J.A.C. Gallas, Lasers, stability, and numbers, *Physica Scripta* **94**, 014003 (2019).
13. J.A.C. Gallas, Orbital carriers and inheritance in discrete-time quadratic dynamics, *Int. J. Mod. Phys. C* **31**, 2050100 (2020).

14. J. Sommer, Vorlesungen über Zahlentheorie (Teubner, Leipzig, 1907).
15. A. Endler and J.A.C. Gallas, Arithmetical signatures of the dynamics of the Hénon map, *Phys. Rev. E* **65**, 036231 (2002).
16. A. Endler and J.A.C. Gallas, Existence and characterization of stable ghost orbits in the Hénon map, *Physica A* **344**, 491-497 (2004).
17. J.A.C. Gallas, Counting orbits in conjugacy classes of the Hénon Hamiltonian repeller, *Phys. Lett. A* **360**, 512-514 (2007).
18. O.J. Brison and J.A.C. Gallas, What is the effective impact of the explosive orbital growth in discrete-time one-dimensional polynomial dynamical systems? *Physica A* **410**, 313-318 (2014).
19. J.A.C. Gallas, Preperiodicity and systematic extraction of periodic orbits of the quadratic map, *Int. J. Mod. Phys. C* **31**, ??? (2020), in print.
20. J.A.C. Gallas, Nonlinear dependencies between sets of periodic orbits, *Europhys. Lett.* **47**, 649-655 (1999).
21. J.A.C. Gallas, Infinite hierarchies of nonlinearly dependent periodic orbits, *Phys. Rev. E* **63**, 016216 (2000).
22. J.P. Tignol, *Galois Theory of Algebraic Equations* (World Scientific, Singapore, 2002).
23. J.A.C. Gallas, Equivalence among orbital equations of polynomial maps, *Int. J. Mod. Phys. C* **29**, 1850082 (2018).
24. S. Pincherle, L'iterazione completa di $x^2 - 2$, *Reale Accad. dei Lincei, Rend. della Classe di Scienze Fisiche, Matematiche e Naturali (Roma)*, Series 5, **29**(1), 329-333 (1920).
25. L.C. Washington, *Introduction to Cyclotomic Fields*, (Springer, New York, 1982).
26. H.M. Edwards, Roots of solvable polynomials of prime degree, *Expo. Math.* **32**, 79-91 (2014).
27. N. Schappacher, On the history of Hilbert's twelfth problem, a comedy of errors. In *Matériaux pour l'Histoire des Mathématiques au XX^e Siècle*. Actes du colloque à la mémoire de Jean Dieudonné. Nice 1996, pp. 243-273. Séminaires et Congrès 3. Paris, Société Mathématique de France.